Title	Charge-discharge Performance of an Ionic Liquid-based Sodium Secondary Battery in a Wide Temperature Range
Author(s)	DING, Changsheng; NOHIRA, Toshiyuki; FUKUNAGA, Atsushi; HAGIWARA, Rika
Citation	Electrochemistry (2015), 83(2): 91-94
Issue Date	2015-02
URL	http://hdl.handle.net/2433/196201
Right	© 2015 The Electrochemical Society of Japan
Type	Journal Article
Textversion	author

Charge-discharge performance of an ionic liquid-based sodium secondary battery in a wide temperature range

Changsheng Ding[a], Toshiyuki Nohira*[a], Atsushi Fukunaga[a,b] and Rika Hagiwara*[a]

[a] Graduate School of Energy Science, Kyoto University, Sakyo-ku, Kyoto 606-8501, Japan.

[b] Electronics & Materials R&D Laboratories, Sumitomo Electric Industries, Ltd., Konohana-ku, Osaka 554-0024, Japan.

* Corresponding authors.

Tel.: +81 75 753 5822;

Fax: +81 75 753 5906.

E-mail addresses: nohira@energy.kyoto-u.ac.jp (T. Nohira)

hagiwara@energy.kyoto-u.ac.jp (R. Hagiwara)

Abstract

A sodium secondary battery has been constructed by using a nonvolatile and nonflammable Na[FSA]-[C_3C_1pyrr][FSA] (FSA = bis(fluorosulfonyl)amide, C_3C_1pyrr = *N*-methyl-*N*-propylpyrrolidinium) ionic liquid, a $NaCrO_2$ positive electrode and a Na metal negative electrode. The charge-discharge performance is evaluated over a wide temperature range of -20~90 ºC. It has been demonstrated that the sodium secondary battery has long cycle lives both at a high temperature of 90 ºC and at a low temperature of 0 ºC. Thus, the ionic liquid-based sodium secondary battery is expected to be a viable alternative to lithium ion battery for many applications.

Keywords*:* Sodium secondary battery; Ionic liquid; Wide operation temperature; Charge-discharge performance

1. Introduction

As post lithium-ion batteries, sodium secondary batteries have been attracting considerable interest because of the low cost and abundant resources of sodium.[1-5] Recently, a number of new electrode active materials have been reported for both positive electrodes (e.g. $Na_4Co_3(PO_4)_2P_2O_7$)[6] and negative electrodes (e.g. amorphous phosphorus–carbon composites)[7]. Moreover, the power density of sodium secondary batteries is anticipated to be

higher than that of lithium-ion batteries because different interactions between sodium-ion and lithium-ions in the host crystal structures can improve the kinetics as well as thermodynamic properties of sodium secondary batteries.[8] Thus, sodium secondary batteries are expected to be utilized for electric vehicles in addition to their intended application of stationary power storage.

For application in electric vehicles, sodium secondary batteries are required to have high energy density, power density, durability, and safety, as well as a wide operating temperature range. However, currently available sodium secondary batteries do not fulfil these requirements completely. The technological bottleneck currently limiting the safety and operating temperature range of sodium secondary batteries is the electrolyte. Therefore, the key to realize improved sodium secondary batteries is to develop a new electrolyte with higher safety and a wider operating temperature range. Conventional organic electrolytes such as $NaClO_4$/propylene carbonate[1,2,9-14] are disadvantageous for the construction of large-scale safe batteries because of their volatility and flammability. Ionic liquids, which are ionic, salt-like materials, generally provide negligibly low volatility, nonflammability, and high thermal and electrochemical stability. Consequently, they have been studied and used as safe electrolytes in many electrochemical fields. An ionic liquid, [C_3C_1pyrr][FSA] (C_3C_1pyrr = *N*-methyl-*N*-propylpyrrolidinium, FSA = bis(fluorosulfonyl)amide), has

been reported to have a low melting point (-9 ºC), high conductivity (6.4 mS cm^{-1} at 25 ºC), and high thermal stability (up to 125 ºC).[15] In addition, we have shown that the ionic liquid, Na[FSA]-[C_3C_1pyrr][FSA], has high ionic conductivity and a wide electrochemical window, and is thus a promising electrolyte for use in sodium secondary batteries.[16] It is expected that a sodium secondary battery based on the Na[FSA]-[C_3C_1pyrr][FSA] ionic liquid electrolyte could be operated over a wide temperature range. In this work, Na[FSA]-[C_3C_1pyrr][FSA] ionic liquid was used as electrolyte, and the charge-discharge performance of Na/$NaCrO_2$ cell was investigated at -20 to 90 ºC.

2. Experimental

Na[FSA] (>99.0%, Mitsubishi Materials Electronic Chemicals) and [C_3C_1pyrr][FSA] (>99.9%, Kanto Chemical Co.) were dried under vacuum at 60 ºC for 24 h. Na[FSA]-[C_3C_1pyrr][FSA] ionic liquid was prepared by mixing Na[FSA] and [C_3C_1pyrr][FSA] with a molar ratio of 2:8 in an Ar-filled glove box. An Na[FSA] concentration of this ionic liquid is 0.998 mol dm^{-3} at 25 ºC. The viscosities at different temperatures of the Na[FSA]-[C_3C_1pyrr][FSA] ionic liquid were measured by a viscometer (Brookfield Engineering Laboratories, DV-IItPRO). The ionic conductivities at different temperatures of the Na[FSA]-[C_3C_1pyrr][FSA] ionic liquid were measured by an AC

impedance method using a calibrated cell with two platinum plate electrodes. The cell constant was determined using standard KCl aqueous solution.

$NaCrO_2$ was prepared by mixing Na_2CO_3 and Cr_2O_3 and calcining the mixture at 850 ºC for 5 h under Ar flow. The composite positive electrode consisted of 80 mass% $NaCrO_2$, 15 mass% acetylene black, and 5 mass% polytetrafluoroethylene, was pressed onto an aluminium mesh current collector and vacuum-impregnated with the Na[FSA]-[C_3C_1pyrr][FSA] ionic liquid. The diameter and thickness of the obtained $NaCrO_2$ electrode were 10 mm and ca. 45 μm, respectively. The loading density of $NaCrO_2$ was 4.7 mg cm^{-2}. Metallic sodium was used as a negative electrode. A glass fibre filter (Whatman, GF-A, 260 mm) was used as a separator that was also vacuum-impregnated with the Na[FSA]-[C_3C_1pyrr][FSA] ionic liquid. R2032-type coin cells were assembled in an Ar-filled glove box. Charge–discharge tests were conducted at constant current rates of 20–2000 mA g^{-1} in the voltage range 2.5–3.5 V at -20~90 ºC. The cycle performance was evaluated at 100 mA g^{-1} at 0 and 90 ºC. AC impedance spectroscopy was carried out for the Na/Na[FSA]-[C_3C_1pyrr][FSA]/$NaCrO_2$ cell over a frequency range of 200 kHz-100 mHz with applied voltage amplitude of 10 mV at an open circuit potential.

3. Results and discussion

The charge–discharge curves of a Na/Na[FSA]-[C_3C_1pyrr][FSA]/$NaCrO_2$ cell tested at -20~90 ºC at a current rate of 20 mA $(g\text{-}NaCrO_2)^{-1}$were shown in Fig. 1a. The testing was performed from 90 ºC to -20 ºC. Several potential plateaus can be observed in both charge

and discharge curves at high operating temperatures, and these potential plateaus disappear gradually with lowering the operating temperature. These potential plateaus correspond to the phase transitions of $Na_{1-x}CrO_2$ ($0 \leq x \leq 0.5$): rhombohedral O3, monoclinic O'3 and monoclinic P'3 structures.[17,18] Fig. 1b shows the differential capacity (dQ/dV) versus voltage plots at 0, 25, 50 and 90 ºC. The dQ/dV curves also clearly show the phase transitions during charge-discharge process. It is interesting to note that the capacity of rhombohedral O3 phase strongly depends on the operation temperature, and that the capacities of monoclinic O'3 and monoclinic P'3 phases are less dependent on the operation temperature. An explanation for this behavior is the subject for a future study.

The variations in the discharge capacity when the temperature is lowered from 90 ºC to -20 ºC are shown in Fig. 1c. At 90 ºC, the discharge capacity is about 118 mAh $(g\text{-}NaCrO_2)^{-1}$ (close to the theoretical capacity of 125 mAh $(g\text{-}NaCrO_2)^{-1}$), which is higher than that of sodium secondary battery with $NaClO_4$ propylene carbonate electrolyte at room temperature (104 mAh $(g\text{-}NaCrO_2)^{-1}$)[17]. The discharge capacity decreases gradually with lowering the operating temperature. At 0 ºC, about 85% of the initial discharge capacity is maintained, and the discharge capacity is similar to that of sodium secondary battery with $NaClO_4$ propylene carbonate electrolyte at room temperature[17]. At a lower temperature of -20 ºC, the cell shows a discharge capacity of about 21 mAh $(g\text{-}NaCrO_2)^{-1}$ in the first cycle, which corresponds to 18% of the

capacity at 90 ºC. When the operation temperature is raised again to 90 ºC, however, the discharge capacity almost fully recovers to the initial value, indicating that no appreciable degradation occurs at the lower temperature. These results indicate that this ionic liquid-based sodium secondary battery can be operated in a wide temperature range from -10 to 90 ºC.

In general, Li-ion batteries using organic electrolytes can be operated between -20 and 60 ºC. However, as the operation temperature increases above 60 ºC, the degradation of Li-ion batteries becomes severe due to the decompositions of SEI layers and electrolytes.[19, 20] The reported sodium secondary batteries based on organic electrolytes were evaluated usually at room temperature.[1,2,9-14] Thus, the operation temperature range of -20~90 ºC for the present sodium secondary battery is wider than those for the reported lithium and sodium secondary batteries utilizing organic electrolytes.

The lower capacity at low temperatures of the ionic liquid-based sodium secondary battery is attributed to the high internal resistance, which may arise from reduced ionic conductivity, limited diffusivity of sodium ions, high electrochemical reaction resistance. For instance, although Na[FSA]-[C_3C_1pyrr][FSA] ionic liquid has high ionic conductivity and low viscosity at high temperatures (15.6 mS cm^{-1} and 16.7 mPs at 80 ºC, respectively), it has lower conductivity and higher viscosity at temperatures below 0 ºC (0.98 mS cm^{-1} and >280 mPs at 0 ºC, respectively). To confirm the effect

of temperature, electrochemical impedance measurements were performed on the Na/Na[FSA]-[C_3C_1pyrr][FSA]/$NaCrO_2$ cell at -20~90 ºC. Fig. 2a shows the Nyquist plots of the cell at -20~90 ºC. The high frequency limit is the ohmic resistance (R_Ω) of which main component is probably the electrolyte resistance. The semicircle at the middle frequency corresponds to the electrochemical reaction process which includes both positive and negative electrode reactions.[21, 22] The electrochemical reaction resistance (R_{ER}) largely increases with lowering the operating temperature, indicating a significant sensitivity to temperature. Fig. 2b shows Arrhenius plots for the reciprocals of R_Ω and R_{ER}. For comparison, an Arrhenius plot for the conductivity (σ) of Na[FSA]-[C_3C_1pyrr][FSA] ionic liquid is also given[16]. Almost similar slopes are observed for R_Ω^{-1} (E_a = 23.0 kJ mol^{-1}) and σ (E_a = 23.7 kJ mol^{-1}), which supports that R_Ω is due to the electrolyte resistance. On the other hand, the slope for R_{ER}^{-1} (E_a = 37.0 kJ mol^{-1}) is different from that for σ. More importantly, the value of R_{ER} is much larger than that of R_Ω, which indicates that the total cell resistance is mainly governed by R_{ER}. In our previous study,[21] the impedance of Na/Na symmetric cell was measured at different temperatures, which revealed that the major component of R_{ER} originates from the Na metal electrode, especially at lower temperatures. Thus, it is concluded that the drastic decrease of capacity at lower temperatures in the present study is mainly caused by the higher R_{ER} of Na counter electrode.

Fig. 3a shows the rate capability of the Na/Na[FSA]-[C_3C_1pyrr][FSA]/$NaCrO_2$ cell at 90 ºC. The discharge capacity at 500 mA $(g\text{-}NaCrO_2)^{-1}$ is 87 mAh $(g\text{-}NaCrO_2)^{-1}$; this value is about 83% of the initial capacity at 50 mA $(g\text{-}NaCrO_2)^{-1}$. Even at a very high rate of 2000 mA $(g\text{-}NaCrO_2)^{-1}$, the cell still maintains a discharge capacity of 45 mAh $(g\text{-}NaCrO_2)^{-1}$, which corresponds to ~42% of the initial capacity. Except for the initial few cycles, the coulombic efficiencies are higher than 99.5%. Thus, the developed cell has practically high rate capability.

The rate capabilities at 0 and 25 ºC were also evaluated and are compared in Fig. 3b. The results clearly show that the cell exhibits better high-rate capability at high operating temperature. At low operating temperature, the ratio of C/C_0 (C: the discharge capacity at a given current rate; C_0: the discharge capacity at a current rate of 20 mA g^{-1}) decreases quickly with an increase in the rate. At 0 ºC, the capacity retention is about 19% and 7% at 500 and 1000 mA $(g\text{-}NaCrO_2)^{-1}$, respectively. The low capacity retention is attributed to the high charge-transfer resistance.

Finally, the cycle performance was investigated. Fig. 4 shows the cycling properties of the sodium battery during charge–discharge tests for 500 cycles at 0 and 90 ºC with a current rate of 100 mA $(g\text{-}NaCrO_2)^{-1}$. At 90 ºC, a reversible capacity of 90 mAh $(g\text{-}NaCrO_2)^{-1}$ is maintained after 500 cycles, and capacity retention is 82%. Except for the initial few cycles, the coulombic efficiencies are higher than 99.8%. Considering

that the upper limit of the operating temperature range for lithium-ion batteries is ~60 ºC, the confirmed stable operation at 90 ºC is an important achievement. Moreover, the safety against an ignition accident is remarkably higher than that in the case of conventional organic electrolytes[1,2,9-14] owing to the nonvolatility and nonflammability of the ionic liquid. At a low operating temperature of 0 ºC, the discharge capacity is almost constant over 500 cycles. The capacity retention reaches as high as ~95% after 500 cycles. The coulombic efficiencies are higher than 99.5% except for the initial few cycles. This proves that the ionic liquid-based sodium battery operates very stably at low temperatures. However, the cycling performance at 90 ºC is inferior to that at 0 ºC, indicating that the degradation at 90 ºC is larger than that at 0 ºC. For practical application, it is necessary to improve the cycling performance of the cell at high temperatures.

4. Conclusions

Na[FSA]-[C_3C_1pyrr][FSA] ionic liquid has been adopted as an electrolyte for a sodium secondary battery. The Na/Na[FSA]-[C_3C_1pyrr][FSA]/$NaCrO_2$ cell can be well operated in a wide temperature range from -10 to 90 ºC. At high operating temperature, the cell exhibits better high-rate capability. The cell is safe and has long cycle lives both at a high temperature of 90 ºC and at a low temperature of 0 ºC. Since the ionic liquid electrolyte possesses intrinsically excellent properties, when higher performance

positive and negative electrodes are developed, this type of sodium secondary battery is well expected to be a viable alternative to lithium-ion batteries for many applications.

Acknowledgement

This work was partly supported by the Advanced Low Carbon Technology Research and Development Program (ALCA) of Japan Science and Technology Agency (JST), and the "Elements Strategy Initiative to Form Core Research Center" (since 2012) of the Ministry of Education, Culture, Sports, Science and Technology (MEXT), Japan.

References

1. R. Berthelot, D. Carlier and C. Delmas, *Nature Mater.*, **10**, 74 (2011).
2. N. Yabuuchi, M. Kajiyama, J. Iwatate, H. Nishikawa, S. Hitomi, R. Okuyama, R. Usui, Y. Yamada and S. Komaba, *Nature Mater.*, **11**, 512 (2012).
3. I. D. Gocheva, M. Nishijima, T. Doi, S. Okada, J. Yamaki and T. Nishida, *J. Power Sources*, **187**, 247 (2009).
4. N. Recham, J. N. Chotard, L. Dupont, K. Djellab, M. Armand and J. M. Tarascon, *J. Electrochem. Soc.*, **156**, A993 (2009).

5. S. Komaba, C. Takei, T. Nakayama, A. Ogata and N. Yabuuchi, *Electrochem. Commun.*, **12,** 355 (2010).

6. M. Nose, H. Nakayama, K. Nobuhara, H. Yamaguchi, S. Nakanishi and H. Iba, *J. Power Sources*, **234**, 175 (2013).

7. J. F. Qian, X. Y. Wu, Y. L. Cao, X. P. Ai and H. X. Yang, *Angew. Chem. Int. Ed.*, **52**, 4633 (2013).

8. S. P. Ong, V. L. Chevrier, G. Hautier, A. Jain, C. Moore, S. Kim, X. H Ma and G. Ceder, *Energy Environ. Sci.*, **4**, 3680 (2011).

9. Y. Yamada, T. Doi, I. Tanaka, S. Okada and J. Yamaki, *J. Power Sources*, **196**, 4837 (2011).

10. Y. Kawabe, N. Yabuuchi, M. Kajiyama, N. Fukuhara, T. Inamasu, R. Okuyama, I. Nakai, and S. Komaba, *Electrochem. Commun.*, **13**, 1225 (2011).

11. S. Wenzel, T. Hara, J. Janek and P. Adelhelm, *Energy Environ. Sci.*, **4**, 3342 (2011).

12. D. H. Kim, S. H. Kang, M. Slater, S. Rood, J. T. Vaughey, N. Karan, M. Balasubramanian and C. S. Johnson, *Adv. Energy Mater.*, **1**, 333 (2011).

13. V. Palomares, P. Serras, I. Villaluenga, K. B. Hueso, J. Carretero-Gonzalez and T. Rojo, *Energy Environ. Sci.*, **5**, 5884 (2012).

14. A. Ponrouch, E. Marchante, M. Courty, J. M. Tarascon and M. R. Palacin, *Energy Environ. Sci.*, **5**, 8572 (2012).

15. Q. Zhou, W. A. Henderson, G. B. Appetecchi, M. Montanino and S. Passerini, *J. Phys. Chem. B*, **112**, 13577 (2008).

16. C. S. Ding, T. Nohira, K. Kuroda, R. Hagiwara, A. Fukunaga, S. Sakai, K. Nitta and S. Inazawa, *J. Power Sources*, **238**, 296 (2013).

17. S. Komaba, T. Nakayama, A. Ogata, T. Shimizu, C. Takei, S Takada, A Hokura, and I Nakai, *ECS Trans.*, **16**, 43 (2009).

18. C.Y. Chen, K. Matsumoto, T. Nohira, R. Hagiwara, A. Fukunaga, S. Sakai, K. Nitta and S. Inazawa, *J. Power Sources*, **237**, 52 (2013).

19. D. Aurbach, Y. Talyosef, B. Markovsky, E. Markevich, E. Zinigrad, L. Asraf, J. S. Gnanaraj, H. J. Kim, *Electrochim. Acta*, **50**, 247 (2004).

20. M. C. Smart, B. V. Ratnakumar, J. F. Whitacre, L. D. Whitcanack, K. B. Chin, M. D. Rodriguez, D. Zhao, S. G. Greenbaum and S. Surampudi, *J. Electrochem. Soc.,* **152**, A1096 (2005).

21. C.Y. Chen, K. Matsumoto, T. Nohira, C.S. Ding, T. Yamamoto, R. Hagiwara, *Electrochim. Acta*, **133**, 583 (2014).

22. T. Shibata, W. Kobayashi, Y. Moritomo, *Appl. Phys. Express*, **6**, 097101 (2013).

Figure captions:

Figure 1. Charge–discharge characteristics of Na/Na[FSA]-[C_3C_1pyrr][FSA]/$NaCrO_2$ cell at -20~90 ºC: (a) Charge–discharge curves, (b) dQ/dV plots, and (c) Discharge capacities. Current rate for charge-discharge cycle: 20 mA (g-$NaCrO_2$)$^{-1}$.

Figure 2. (a)Nyquist plots for a Na/Na[FSA]-[C_3C_1pyrr][FSA]/ $NaCrO_2$ cell at -20~90 ºC. (b) Arrhenius plots for the reciprocals of ohmic resistance (R_Ω) and electrochemical reaction resistance (R_{ER}). An Arrhenius plot for the conductivity (σ) of Na[FSA]-[C_3C_1pyrr][FSA] ionic liquid is also shown for comparison.

Figure 3. (a) Rate capability of Na/Na[FSA]-[C_3C_1pyrr][FSA]/$NaCrO_2$ cell at 90 ºC. (b) The comparison of rate performance at 0, 25 and 90 ºC. The current rates for charge–discharge cycles were 50–2000 mA (g-$NaCrO_2$)$^{-1}$.

Figure 4. Cycle performance of Na/Na[FSA]-[C_3C_1pyrr][FSA]/$NaCrO_2$ cell at 0 and 90 ºC. The current rate for charge–discharge cycles was 100 mA (g-$NaCrO_2$)$^{-1}$.

(a)

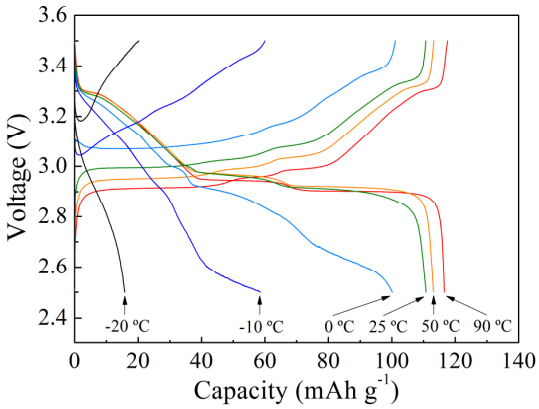
Voltage (V)
Capacity (mAh g-1)
-20 ºC
-10 ºC
0 ºC
25 ºC
50 ºC
90 ºC

(b)

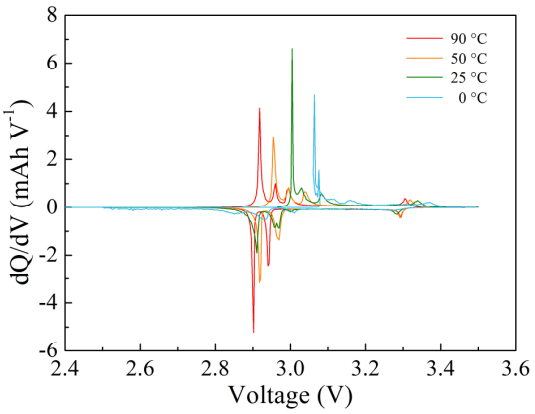
dQ/dV (mAh V-1)
Voltage (V)
90 °C
50 °C
25 °C
0 °C

(c)

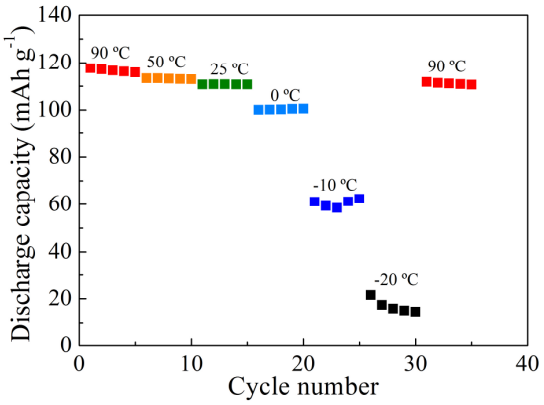
Discharge capacity (mAh g-1)
Cycle number
90 ºC
50 ºC
25 ºC
0 ºC
-10 ºC
-20 ºC
90 ºC

Fig. 1

(a)

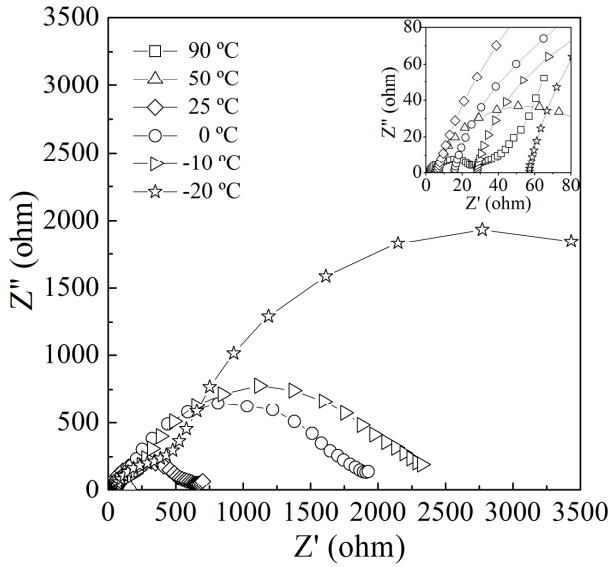
90 ºC
50 ºC
25 ºC
0 ºC
-10 ºC
-20 ºC
Z'' (ohm)
Z' (ohm)
0
500
1000
1500
2000
2500
3000
3500
Z'' (ohm)
Z' (ohm)
0
20
40
60
80

(b)

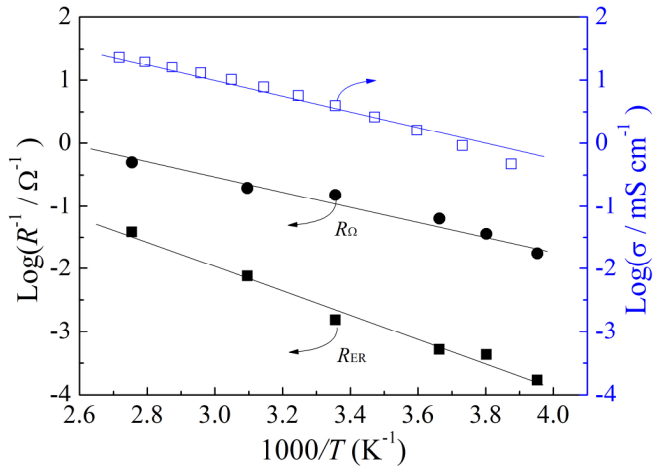
Log(R^-1 / Ω^-1)
Log(σ / mS cm^-1)
1000/T (K^-1)
RΩ
RER
2.6
2.8
3.0
3.2
3.4
3.6
3.8
4.0
2
1
0
-1
-2
-3
-4

Fig. 2

(a)

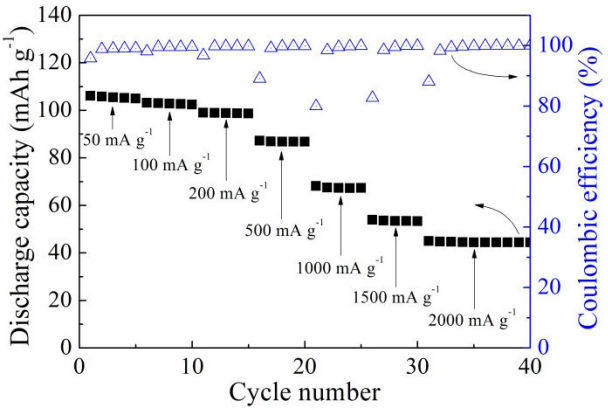
Discharge capacity (mAh g-1)
Coulombic efficiency (%)
Cycle number
50 mA g-1
100 mA g-1
200 mA g-1
500 mA g-1
1000 mA g-1
1500 mA g-1
2000 mA g-1

(b)

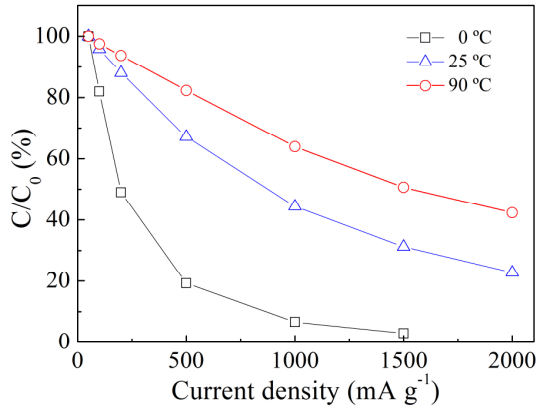
C/C0 (%)
Current density (mA g-1)
0 °C
25 °C
90 °C

Fig. 3

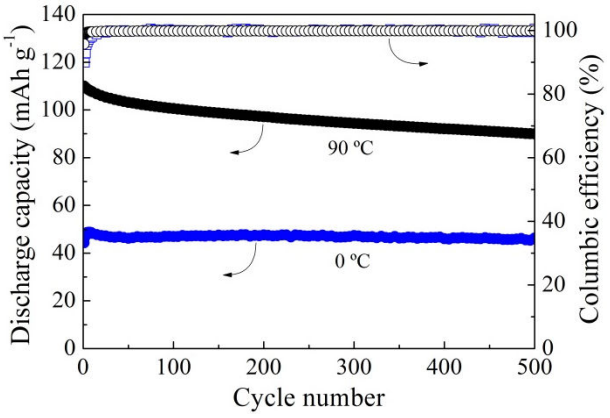
Discharge capacity (mAh g-1)
Columbic efficiency (%)
Cycle number
90 ºC
0 ºC
0
20
40
60
80
100
120
140
0
100
200
300
400
500

Fig. 4